Available online at www.sciencedirect.com
ScienceDirect
Micron 38 (2007) 49–57
micron
www.elsevier.com/locate/micron

Ultrastructural and functional characterization of circulating hemocytes from the freshwater crayfish *Astacus leptodactylus*: Cell types and their role after in vivo artificial non-self challenge

Piero Giulio Giulianini *, Manuel Bierti, Simonetta Lorenzon [1], Silvia Battistella, Enrico Antonio Ferrero

Department of Biology, University of Trieste, via Licio Giorgieri 7, I-34127 Trieste, Italy

Received 20 January 2006; received in revised form 30 March 2006; accepted 30 March 2006

Abstract

The freshwater crayfish *Astacus leptodactylus* (Eschscholtz, 1823) is an important aquacultured decapod species as well as an invasive species in some European countries. In the current investigation we characterized the different classes of circulating blood cells in *A. leptodactylus* by means of light and electron microscopy analysis and we explored their reaction to different latex beads particles in vivo by total and differential cell counts at 0.5, 1, 2 and 4 h after injections. We identified hemocytes by granule size morphometry as hyaline hemocytes with no or rare tiny granules, small granule hemocytes, unimodal medium diameter granule hemocytes and both small and large granule containing hemocytes. The latter granular hemocytes showed the strongest phenoloxidase L-DOPA reactivity both in granules and cytoplasm. *A. leptodactylus* respond to foreign particles with strong cellular immune responses. All treatments elicited a total hemocyte increase with a conspicuous recruitment of large granule containing hemocytes. All hemocyte types mounted some phagocytic response but the small granule hemocytes were the only ones involved in phagocytic response to all foreign particles with the highest percentages. These results (1) depict the variability in decapod hemocyte functional morphology; (2) identify the small granule hemocyte as the major phagocytic cell; (3) suggest that the rather rapid recruitment of large granule hemocyte in all treatments plays a relevant role by this hemocyte type in defense against foreign particles, probably in nodule formation.

Keywords: Hemocytes; Ultrastructure; Latex beads; Phagocytosis; Cellular immunity; *Astacus leptodactylus* (Crustacea)

1. Introduction

The circulating hemocytes of crustaceans play a central role in innate immunity. They are involved in nodule formation, encapsulation and in phagocytosis. Three hemocyte types are commonly described in crustaceans: hyaline hemocytes (agranular), small granule (semigranular) hemocytes, and large granule (granular) hemocytes (Mix and Sparks, 1980; Bauchau, 1981; Söderhäll and Smith, 1983; Martin and Graves, 1985; Hose et al., 1990; Johansson et al., 2000; Battison et al., 2003). The morphological classes are essentially based on granule number and size and on nucleus to cytoplasm ratio by using phase contrast or brightfield light microscopy and transmission electron microscopy. Martin and Graves (1985) pointed out that routine staining procedures of hemolymph smears are not useful because they are often ambiguous, not easily duplicated and the cell morphology is highly distorted. Recently, drawbacks induced by different light microscopy techniques on live cells and staining of unfixed hemolymph smears have been overpassed by authors that used cytocentrifugation of diluted fixed hemolymph followed by Wright-Giemsa staining and obtaining permanent stained slides (Horney et al., 2002; Battison et al., 2003). The latter technique allowed discrimination of 11 hemocyte types, enabling to observe less mature hemocytes in late stages of *Aerococcus viridans* var. *homari* infection (Battison et al., 2003). The number of circulating hemocytes is also important and it can decrease dramatically after bacterial infection or following various types of stresses (Lorenzon et al., 2001, 2002).

The freshwater crayfish *Astacus leptodactylus* (Eschscholtz, 1823) is an economically important aquacultured species as well as an invasive species in some European countries. The cellular immune response of *A. leptodactylus* has gone

* Corresponding author. Tel.: +39 040 5583560; fax: +39 040 575079.
E-mail address: giuliani@units.it (P.G. Giulianini).
[1] Present address: Osservatorio Geofisico Sperimentale, Dipartimento di Oceanografia Biologica, via Picard, 54, I-34010 Trieste, Italy.

0968-4328/$ – see front matter
doi:10.1016/j.micron.2006.03.019

essentially unstudied. The aim of the current investigation is the characterization, not subject to procedural variations and subjective interpretation of the different classes of blood cells in *A. leptodactylus* by means of light and electron microscopy quantitative analysis and the exploration of their acute responses to foreign particles in vivo whereas phagocytosis assays in crustaceans are usually performed in vitro with consequent cell adhesion and altered morphology (Hose et al., 1990; Gargioni and Barracco, 1998; Sung and Ru Sun, 2002). Moreover in these studies administered foreign particles vary from natural ones like bacteria and yeast (Hose et al., 1990; Gargioni and Barracco, 1998) to, more recently, artificial ones like latex beads (Sung and Ru Sun, 2002). We decided to use either unmodified or carboxylated latex beads with different diameters as standardized foreign particles as they are widely used for phagocytosis assays in arthropods (Chang et al., 2000; Giulianini et al., 2003; Hillyer et al., 2003a,b). Moreover, as for most crustacean species the variations in total and differential hemocytes count (THC, DHC) values are quite high among individual animals (Johansson et al., 2000; Sung and Ru Sun, 2002), we decided to perform THC and DHC time course on single treated animals.

2. Materials and methods

2.1. Experimental animals

The crayfish *A. leptodactylus* (Decapoda, Astacidea) were imported from Turkey by a local dealer. Animals were stocked in 120 l glass tanks with closed circuit filtered and thoroughly aerated freshwater 16–18 °C, and with natural photoperiod condition. Forty-eight hours before experiments, each animal was marked for individual recognition and kept unfed until the end of the experiments. Hard-shelled, intermolt apparently healthy male crayfish were selected for experiments.

2.2. Light and transmission electron microscopy

Two hundred microlitres hemolymph samples (about 2×10^5 hemocytes counted by using a Bürker's chamber) were drawn from the pericardial sinus of each animal into a sterile plastic 1 ml syringe (26-gauge needle) filled with an equal volume of fixative (2.5% glutaraldehyde, 1% paraformaldehyde, 7.5% saturated picric acid solution in 0.1 M cacodylate buffer pH 7.4) and, after a fixation for a minimum of 10 min, the hemocytes were pelleted in 1 ml of fixative by 14,000 rpm centrifugation for 10 min at 20 °C. The pellets obtained were then washed in 0.1 M cacodylate buffer pH 7.4 and post-fixed in 1% osmium tetroxide in the same buffer, serially dehydrated in ethanol and embedded, via propylene oxide, in Embed812/Araldite (Electron Microscopy Sciences, Fort Washington, PA) or, without post-fixation, they were serially dehydrated in ethanol and embedded in LR-White (Sigma). For light microscopy, sections 2 μm thick were collected on slides, baked for 5 min at 80 °C and stained with 0.5% toluidine blue in 0.1% carbonate solution at pH 11.1 at the same temperature. For TEM, silver/gold-coloured sections were stained with uranyl acetate and lead citrate and observed with a TEM Philips EM 208. For phenoloxidase (PO) activity assessment the hemocytes were fixed in 1% glutaraldehyde, 1% paraformaldehyde in 0.15 M sterile phosphate buffered saline pH 7.4 (PBS, Sigma) for 10 min at 20 °C. The cells were maintained in suspension by means of vortexing and continuous rotation of the eppendorf plastic tube. After three rinsing in PBS (15 min each), the cell suspension was incubated in 0.1% L-DOPA (Sigma) in PBS for 16 h at 20 °C. The hemocytes were then pelleted by 14,000 rpm centrifugation for 10 min at 20 °C, and embedded, as described above (without osmium tetroxide post-fixation), in Embed812/Araldite. Silver/gold-coloured unstained sections were observed with a TEM Philips EM 208. Electron-density of granules and cytoplasm was interpreted as a positive reaction. A parallel control of hemocytes fixed, embedded and observed as described above, but incubated in PBS without L-DOPA, did not show any electron-density.

2.3. In vivo phagocytosis assay

In the pericardial sinus of the crayfish were injected with a 26-gauge needle 200 μl of: (1) sterile PBS; equal amounts of (2) polystyrene latex beads 1.1 μm in diameter (approximately 5×10^8 beads); (3) polystyrene latex beads 3.0 μm in diameter; (4) carboxylated polystyrene latex beads 0.9 μm in diameter; (each of them aqueous suspension, 10% solids content, Sigma) diluted 1:1 in 0.15 M PBS. For total hemocyte counts (THC) 50 μl of hemolymph from each animal of groups of six crayfish were collected after 0.5, 1, 2, 4, 6 and 24 h and hemocytes counted using a Bürker's chamber. For differential hemocyte counts (DHC), after 0.5, 1, 2, 4 h 200 μl of hemolymph were processed as described above for light and electron microscopy. Three differential cell counts were made by two different operators from 2 μm semithin transverse sections of the full pellet thickness stained with toluidine blue. A total of 645–1126 cells were scored from three slides per pellet. Neither aggregate latex beads nor aggregate cells were found in the pellets. As a control, non-injected animals were bled at the same times and in the same way as the experimental groups in order to evaluate bleeding and manipulation stresses (''none'' group in Fig. 1).

2.4. Image and statistical analysis

For light microscopy, selected areas were observed with an Olympus BX50 microscope, and images were acquired with an Olympus DP11 photo camera at a resolution of 1712 × 1368 pixels. For TEM, negative plates were digitised with an Epson Photo Perfection scanner at 1200 dpi (optical resolution) and saved as a Tagged Image Format file. All measurements, statistical analyses and photocomposition were performed with an Image-Pro Plus 4.5 Software (Media Cybernetics, Silver Spring, MD). The automatic granule measurements were made on digitised TEM plates using the mean diameter function: ''average length of diameters measured at 2° intervals and passing through object's centroid'' (Image Pro Plus software). Granule mean diameter distributions were tested for normality

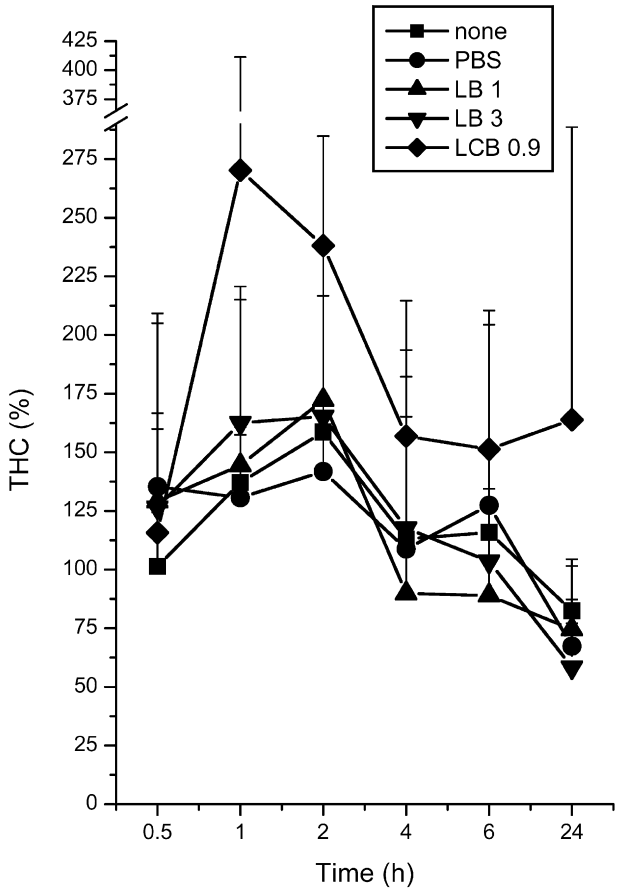

Fig. 1. Variation of total circulating hemocytes percentage (THC %) over initial values in *A. leptodactylus* groups at increasing time after injection of: phosphate buffered saline (PBS), 1 μm diameter latex beads (LB 1), 3 μm diameter latex beads (LB 3), and 0.9 μm diameter carboxylate-modified latex beads (LBC 0.9). As a control, non-injected animals were bled at the same times and in the same way as the experimental groups in order to evaluate bleeding and manipulation stresses (none group). The initial number of circulating hemocytes is $1.14 \pm 0.53 \times 10^6$/ml ($n = 45$). Values are expressed as means ± S.D. ($n = 6$).

(test K-S, test of Lilliefors). For normal distributions comparisons, after Levene test for variance homogeneity, we used parametric statistic (two tailed *t*-test) whereas for non-normal distributions comparisons we used non-parametric test (Mann–Whitney test).

3. Results

Within a continuum of granule occurrences and size *A. leptodactylus* hemocytes were classed as hyaline hemocytes (HH) with no or rare tiny granules, small granule hemocytes (SGH), unimodal medium diameter granule hemocytes (MGH) and both small and large granule containing hemocytes (LGH). Relative percentages of these hemocyte morphotypes from untreated *A. leptodactylus* are summarized in Table 1.

3.1. Hyaline hemocytes

They are the smallest circulating hemocytes with an oval/irregular profile and a mean diameter of 10.3 ± 1.5 μm ($n = 8$); they are characterized by a high nucleus/cell surface ratio of about 0.54 (Fig. 2A–C). The nucleus, euchromatic and sometimes lobated, is located in a central position and it presents large chromatin lumps. The cytoplasm shows free polyribosomes, rough endoplasmic reticulum and few (up to 20 per cell section) small electron dense vesicles about 0.3 μm in diameter. The HHs show faint PO L-DOPA reactivity in the cytoplasm (Fig. 5A).

3.2. Small granule hemocytes

They present an elongated oval/circular profile with a mean diameter of 15.6 ± 3.4 μm ($n = 10$; Fig. 2B and C). The large nucleus is located in a central position with an irregular, sometimes lobated and polymorphic profile. The cytoplasm presents a well-developed rough endoplasmic reticulum, golgi complex and small (about 0.5 μm in diameter) round to elongated mitochondria with tabular cristae (Fig. 2C). They are characterized by numerous electron dense granules (up to 100 per cell section) with a round to elliptical profile and a mean diameter of 0.38 ± 0.15 μm ($n = 91$; Figs. 2C and 3A). The SGHs show weak PO L-DOPA reactivity in the granules but not in the cytoplasm (Fig. 5A).

3.3. Unimodal medium granule size hemocytes

These hemocytes show a circular and occasionally irregular profile with a mean diameter of 14.9 ± 1.2 μm ($n = 8$; Fig. 2D and E). The euchromatic nucleus, mainly located in an eccentric position, presents a circular/irregular profile. The cytoplasm presents a well-developed rough endoplasmic reticulum, golgi complex and small round to elongated mitochondria (Fig. 2E) with tabular cristae. They are characterized by variable electron dense granules with mainly a round profile and a mean diameter of 0.80 ± 0.37 μm ($n = 60$; Figs. 2E and 3B). This hemocyte type is not detectable in traditional unfixed preparations observed with Nomarsky's contrast while it is easily appreciable in stained semithin pellet sections (Fig. 2D). The MGHs show the granules clearly positive for PO L-DOPA reactivity (Fig. 5C).

3.4. Large and small granule hemocytes

They present a circular to spindle shaped profile with a mean diameter of 21.3 ± 5.2 μm ($n = 10$) but reaching a maximum diameter of about 44 μm (Fig. 3A–D). The nucleoplasm is finely dispersed with some chromatin lumps mainly located beneath the nuclear envelope. These hemocytes are characterized by large, electron-dense, structure-less, membrane-enclosed granules showing a round to oval or lemon-like granule profile with a maximum diameter up to 3.1 μm (Fig. 3A). A second class of small electron-dense granules irregular in shape is also present (Fig. 3A). Computer aided automatic measurements easily allow to discriminate the two populations of granules: one with a mode of 0.2–0.4 μm (mean 0.56 ± 0.29, $n = 95$) and

Table 1
Variation of hemocyte types percentage in *A. leptodactylus* hemocytes pellet sections at increasing time (30 min, 1, 2, and 4 h) after injection of phosphate buffered saline (PBS), 1 μm diameter latex beads (LB1), 3 μm diameter latex beads (LB3) and 0.9 μm diameter carboxylate-modified latex beads (LBC0.9)

Treatment Time	HH	SGH	MGH	LGH	Phagocyting HH	Phagocyting SGH	Phagocyting MGH	Phagocyting LGH
none	46.7±2.9	31.8±2.5	4.4±0.6	17.1±3.2				
PBS 30'	31.8±1.6	24.7±0.2	6.9±0.2	36.5±2.1				
PBS 1h	27.5±9.5	17.7±1.2	7.6±2.1	47.2±12.2				
PBS 2h	39.9±6.6	18.2±5.6	3.6±0.7	38.3±7.6				
PBS 4h	25.3±1.5	37.0±5.0	4.6±0.4	33.1±4.2				
LB1 30'	27.9±0.3	17.9±0.6	8.6±0.3	44.0±0.9		1.3±0.5		0.4±0.5
LB1 1h	32.5±6.1	23.4±1.7	4.5±1.6	36.7±4.3	0.6±0.5	2.3±1.3		
LB1 2h	11.9±0.3	15.5±5.2	5.8±1.9	62.6±8.3	0.1±0.2	3.6±1.1	0.4±0.7	
LB1 4h	24.4±1.2	25.4±2.8	4.0±1.6	43.5±2.0		2.4±0.1	0.3±0.2	
LB3 30'	32.3±1.6	23.1±5.0	4.0±0.9	40.6±4.6				
LB3 1h	40.6±4.8	29.9±4.2	3.9±0.6	24.1±1.0	0.1±0.2	1.5±0.4		
LB3 2h	38.1±1.4	19.3±0.3	4.0±0.4	38.0±1.3		0.2±0.4	0.4±0.5	
LB3 4h	31.6±2.7	26.7±5.1	4.5±0.6	36.1±5.2		1.2±1.0		
LBC0.9 30'	31.3±4.1	27.7±2.7	6.0±0.8	33.9±0.3		1.2±0.4		
LBC0.9 1h	17.2±2.6	14.5±0.5	4.8±0.5	62.7±3.6		0.6±0.6		0.1±0.2
LBC0.9 2h	15.6±1.2	19.8±3.3	5.2±0.9	58.6±4.7		0.7±0.2		
LBC0.9 4h	18.6±2.6	15.8±2.2	4.5±0.3	57.7±1.5	1.4±1.5	2.0±0.3		

The initial percentages from untreated *A. leptodactylus* are boxed (none group). The lowest hyaline and small granule hemocyte percentages and the highest large granule hemocyte percentages are highlighted in grey. Values are expressed as means ± S.D. ($n = 6$).

the second with a mode of 1.6–1.8 μm (mean 1.76 ± 0.35, $n = 23$). Bundles of microtubules running parallel just beneath the plasma membrane are present (Fig. 3A). During defensive response to injected latex beads, plasma membrane ruptures, electron lucent vacuoles, and a nucleus with electron lucent nucleoplasm and heterochromatic lumps were observed in LGH (Fig. 3C). Interestingly, only this ''senescent'' LGH presents the larger granules with electron lucent spots and merging with each other (Fig. 3C). Sections of pellet embedded in LR-white without osmium post-fixation allow distinguishing two subpopulations: LGH with larger granules intensely stained with toluidine blue and LGH with larger granules presenting a pale staining (Fig. 3D). The class of smaller granules maintains its staining characteristics.

The morphometric statistical analysis underlying differential hemocyte characterization is reported in Fig. 4. The mean diameter frequency distributions of granules in SGH, MGH and LGH hemocytes are shown in Fig. 4. The SGH granules mean diameters significantly differ from granules mean diameters of MGH (Mann–Whitney test: $n_{SGH} = 91$, $n_{MGH} = 60$, $Z = 7.28$, $P < 0.0001$). The two classes of diameter frequencies of LGH granules are significantly different (Mann–Whitney test: $n_1 = 94$, $n_2 = 23$, $Z = 7.41$, $P < 0.001$). Moreover, the larger class of LGH granules mean diameters significantly differ from granules mean diameters of MGH (t test: $t = 10.79$, gl = 81, $P < 0.001$) and SGH (Mann–Whitney test: $n_{LGH} = 23$, $n_{SGH} = 91$, $Z = 7.39$, $P < 0.001$).

The LGHs show always a PO L-DOPA reactivity: the granules are dark stained and the cytoplasm reveals weak (Fig. 5C) to very intense staining (Fig. 5A and B).

3.5. *In vivo phagocytosis assay: morphology, total and differential cell counts*

The variations of circulating hemocytes percentages over initial values in the control group and in the four experimental groups after injections are summarized in Fig. 1. In all treatments the maximum THC increases were observed at 2 h after injections except for carboxylated latex particles that show at 1 h the highest THC recorded in the experiments (270.23 ± 141.12).

The percentages of hemocyte types, counted using light microscopy of 2 μm semithin sections of pellets, after the four in vivo treatments are summarized in Table 1. In all treatments HH percentage, that show the highest percentage in untreated animals (46.7 ± 2.9), decreases consistently to lower values and to a minimum of 11.9 ± 0.3 1 h after injection of 1 μm latex beads. The SGH DHC percentages decrease in all the treatments (except for 4 h PBS) from the initial values of 31.8 ± 2.5, reaching a minimum of 14.5 ± 0.5 after 1 h post injection of 0.9 μm carboxylated latex beads. The MGH DHC percentages remain almost the same in all treatments reaching a maximum after 30 min post injection of 1 μm latex beads (from 4.4 ± 0.6 to 8.6 ± 0.3). The LGH DHC (17.1 ± 3.2 in untreated animals) increase consistently in all the treatments reaching the highest values of 62.7 ± 3.6 and 62.6 ± 8.3 after 1 and 2 h post injection of respectively 1 μm latex beads and 0.9 μm carboxylated latex beads. The main phagocyting activity is shown by SGH that phagocytize all foreign particle types reaching a maximum of 3.6 ± 1.1% of total hemocytes with 1 μm latex particles 2 h after injection. The other hemocyte types show a weak phagocytic activity (except for

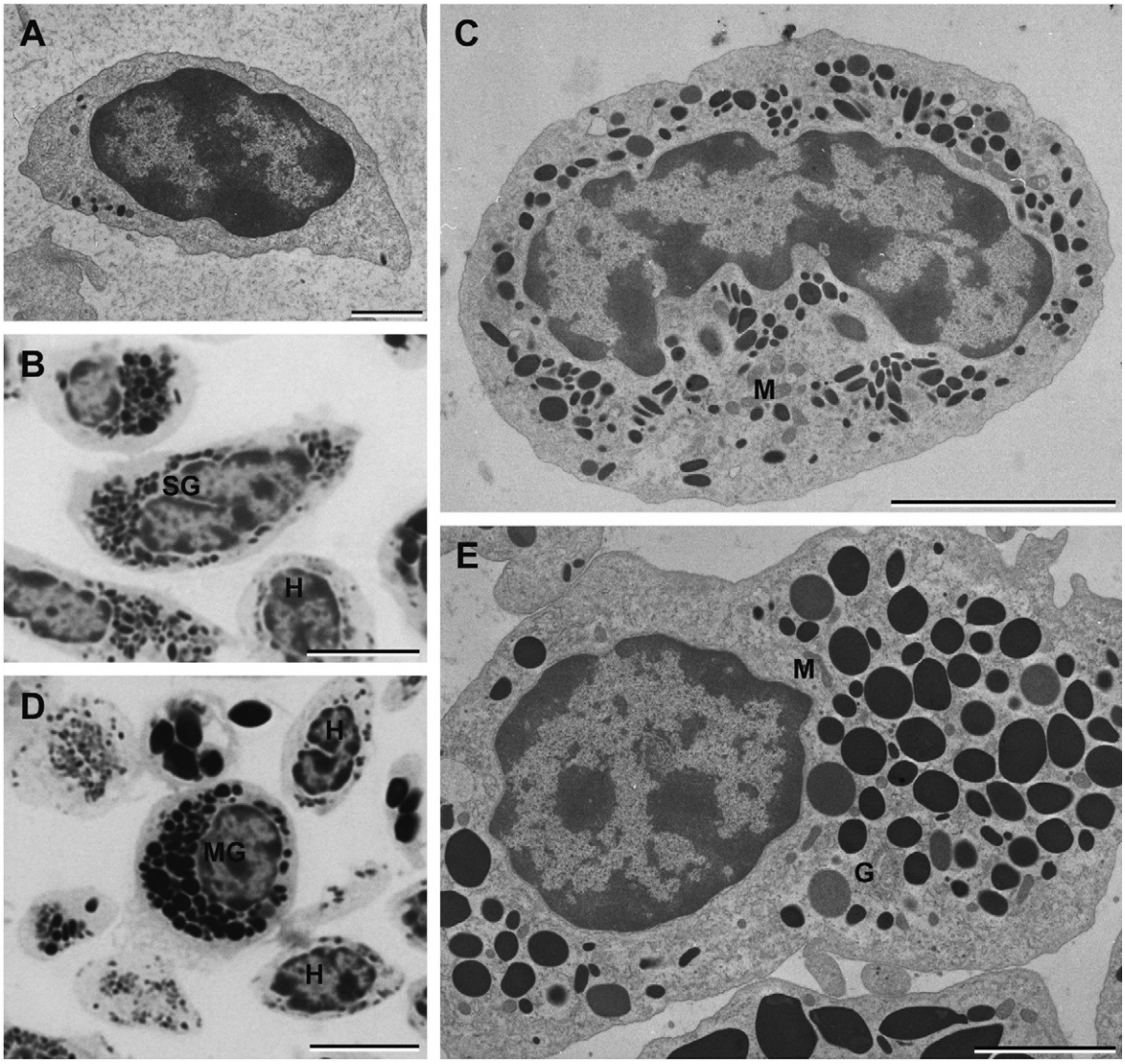

Fig. 2. Transmission electron microscopy of *A. leptodactylus* hemocytes. (A) Hyaline hemocyte showing a high nucleus/cell ratio. (C) Small granule hemocyte. (E) Medium granule hemocyte filled with the typical granules. Light microscopy semithin sections of *A. leptodactylus* hemocytes. G: golgi complex; H: hyaline hemocyte; M: mitochondrion; MG: medium granule hemocyte; SG: small granule hemocyte. Scale bars 2 μm (A), 10 μm (B and C), 5 μm (D), 4 μm (E).

HH with carboxylated latex beads) always in less than 1% of total hemocytes.

Activated phagocyting SGH are still characterized by an eccentric euchromatic nucleus and by granules with variable electron-density and profile (Fig. 6A). Some electro-lucent large vacuoles are present in the cytoplasm (Fig. 6A). After carboxylated latex beads injection a small number of LGH that present conspicuous phagocytic activity were observed (Fig. 6B). Their cytoplasm is filled with latex beads and they show plasma membrane ruptures, a heterochromatic nucleus and complex heterogeneous electron-dense large vacuoles and merging granules with clear spots (Fig. 6B).

4. Discussion

The present study uses light-/electron-microscopy on hemocyte sections and fresh hemocyte counts combined approaches to investigate the circulating hemocytes of a freshwater decapod crustacean species after artificial immune challenge. It allows the description of crayfish circulating hemocytes morphology when unchallenged and when involved in phagocytic activity as well as the definition of its time course. The traditional morphological hemocyte classification is based essentially on arbitrary thresholds of granule number and size and of nucleus to cellular ratio using phase contrast or brightfield light microscopy and transmission electron microscopy. Conventionally three hemocyte types are described in crustaceans: hyaline hemocytes (agranular), small granule (semigranular) hemocytes, and large granule (granular) hemocytes (Mix and Sparks, 1980; Bauchau, 1981; Martin and Graves, 1985; Hose et al., 1990; Gargioni and Barracco, 1998; Johansson et al., 2000; Sung and Ru Sun, 2002; Battison et al., 2003). In order to characterize the circulating hemocytes of the freshwater crayfish *A. leptodactylus* ultrastructural features of circulating hemocytes were automatically analysed by means of image-analysis software and the measurements

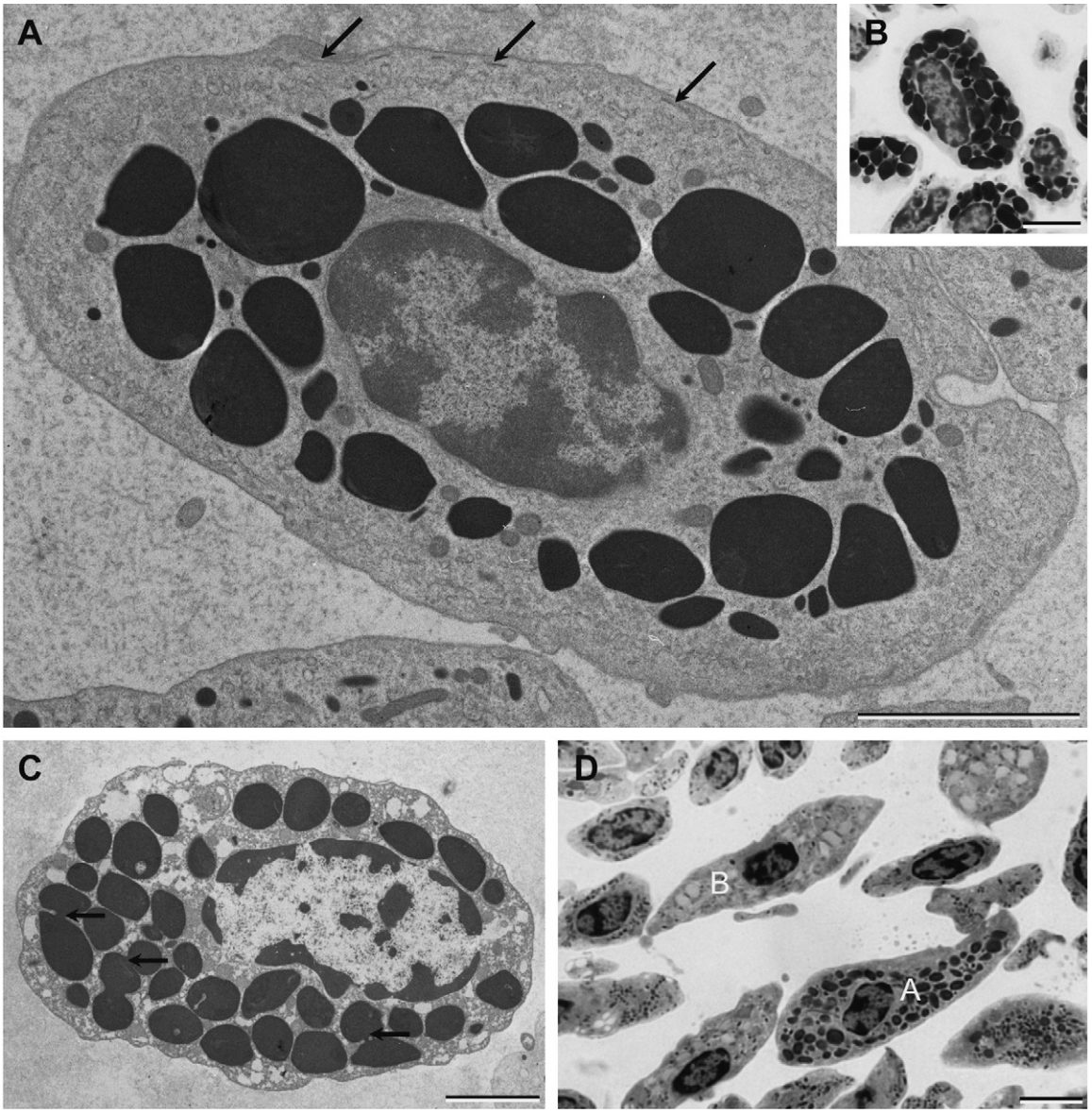

Fig. 3. Transmission electron microscopy of *A. leptodactylus* hemocytes. (A) Large granule hemocyte. Note the bundles of microtubules running parallel just beneath the plasma membrane (arrows). (C) Large granule hemocyte showing "senescent" features. Note the large granules merging each other (arrows). Light microscopy semithin sections of *A. leptodactylus* hemocytes. (B) Large granule hemocyte. (D) Large granule hemocytes showing intensely stained granules (A) and poorly stained granules (B) without osmium tetroxide post-fixation. Scale bars 4 μm (A and C), 10 μm (B and D).

compared for significant differences. Moreover we combined traditional THC on unfixed hemolymph samples to DHC on semithin sections of resin-embedded pellets from hemocytes immediately fixed in the syringe during bleeding. This method allows us to further characterize morphotypes easily detectable in semithin section at light microscopical level (Fig. 2D) and identify a medium diameter granule hemocytes that represents about 4% of total circulating hemocyte. The characterization of this intermediate hemocyte form is well supported by statistical analysis of the granule diameters; in fact the average granules diameters of the MGH differ significantly from those of SGH and LGH (for both $p < 0.001$ at least).

It is not the intent of the present study to discuss the hypothetical maturation sequence of *A. leptodactylus* hemocytes, but the ultrastructural features suggest that HH are a relatively undifferentiated hemocyte type with a central nucleus, a high nucleus/cell ratio, and a cytoplasm with scanty organelles and the few granules similar in diameter to those of SGH. On the contrary SGH shows features of a well-differentiated hemocyte type with a polymorphic nucleus and well-developed organelles. The SGH are also involved primarily in phagocytic activity. The round and eccentric nucleus of MGH is evidently different from that of SGH. The LGH also shows features of a well-differentiated hemocyte type. Besides they are the only hemocyte type that shows evident different stages of maturation, with at least two subpopulations found without osmium tetroxide post-fixation supporting a different composition of lipid and protein content

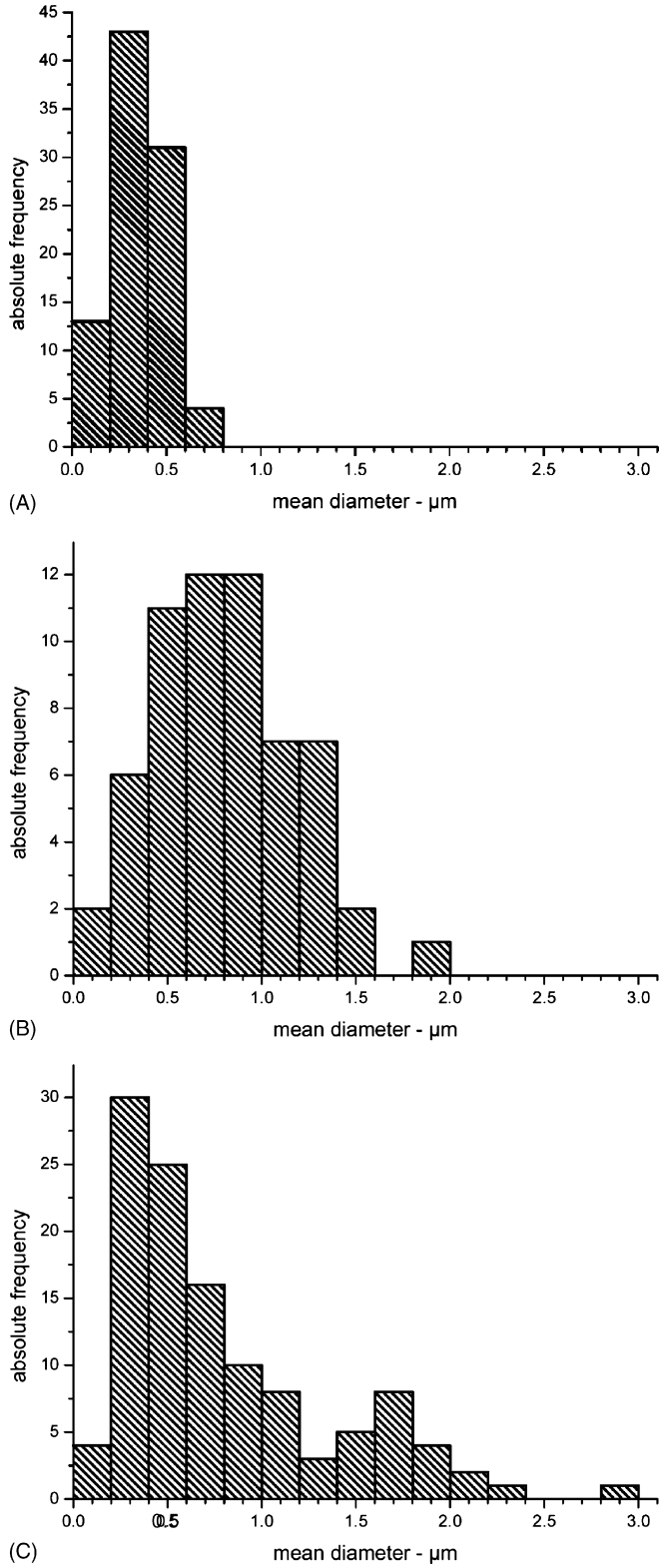

Fig. 4. Distribution of granules mean diameter automatic measurements of *A. leptodactylus* hemocytes. (A) Small granule hemocyte granules ($n = 91$). (B) Medium granule hemocytes granules ($n = 60$). (C) Large granule hemocytes granules ($n = 118$).

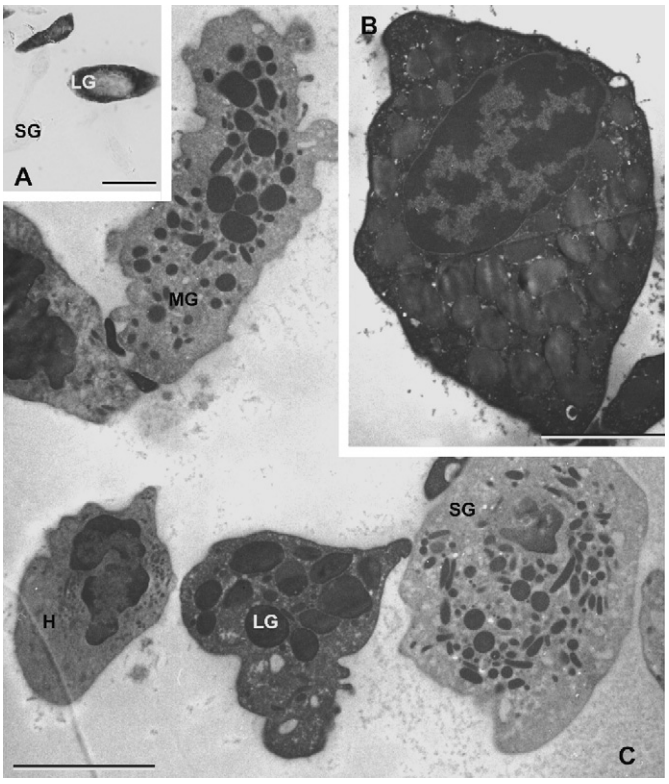

Fig. 5. Light (A), and transmission electron microscopy (B and C) of *A. leptodactylus* hemocytes treated with L-DOPA for the PO presence. (A and B) The large granule hemocytes show sometimes a cytoplasm with strong positive staining. At light microscopy level small granule hemocyte (SG) show faint PO L-DOPA reactivity. (C) At ultrastructural level can be noted: the positive staining of the granules of small granule hemocyte (SG), medium granule hemocyte (MG), and large granule hemocyte (LG). The hyaline hemocyte shows weak cytoplasm staining (H). Scale bars 10 µm (A), 3 µm (B) and 5 µm (C).

in the larger granule classes (Fig. 2D), and a ''senescent'' stage after activation (Fig. 3C). Moreover their rapid and massive recruitment suggests a well-defined functional role and that LGH differentiation process usually occurs in the hematopoietic tissue or marginal compartments. In conclusion, these findings suggest that the only hypothetical maturation sequence could be HH-SGH. Further study on the hematopoietic tissues of *A. leptodactylus* would elucidate if MGH could be immature LGH released in the hemolymph stream.

In *Astacus astacus* and in *Carcinus maenas* the PO occurrence, revealed with L-DOPA, is present in the granular and semigranular cells (Smith and Söderhäll, 1983; Söderhäll and Smith, 1983). In *Homarus americanus*, *Panulirus interruptus* and *Loxorhynchus grandis* the PO occurrence was restricted to SGH and LGH, with the highest activity of the latter hemocyte type (Hose et al., 1990). In *Penaeus paulensis* PO activity was found primarily within the hemocyte lysate supernatant (Perazzolo and Barracco, 1997). More recently in *Pacifastacus leniusculus* was demonstrated, by means of in situ hybridisation, the prophenoloxidase transcript in the circulating hemocytes but not in the cells of hematopoietic tissue suggesting that the final stage of development of functional semigranular or granular hemocytes occurs after their release

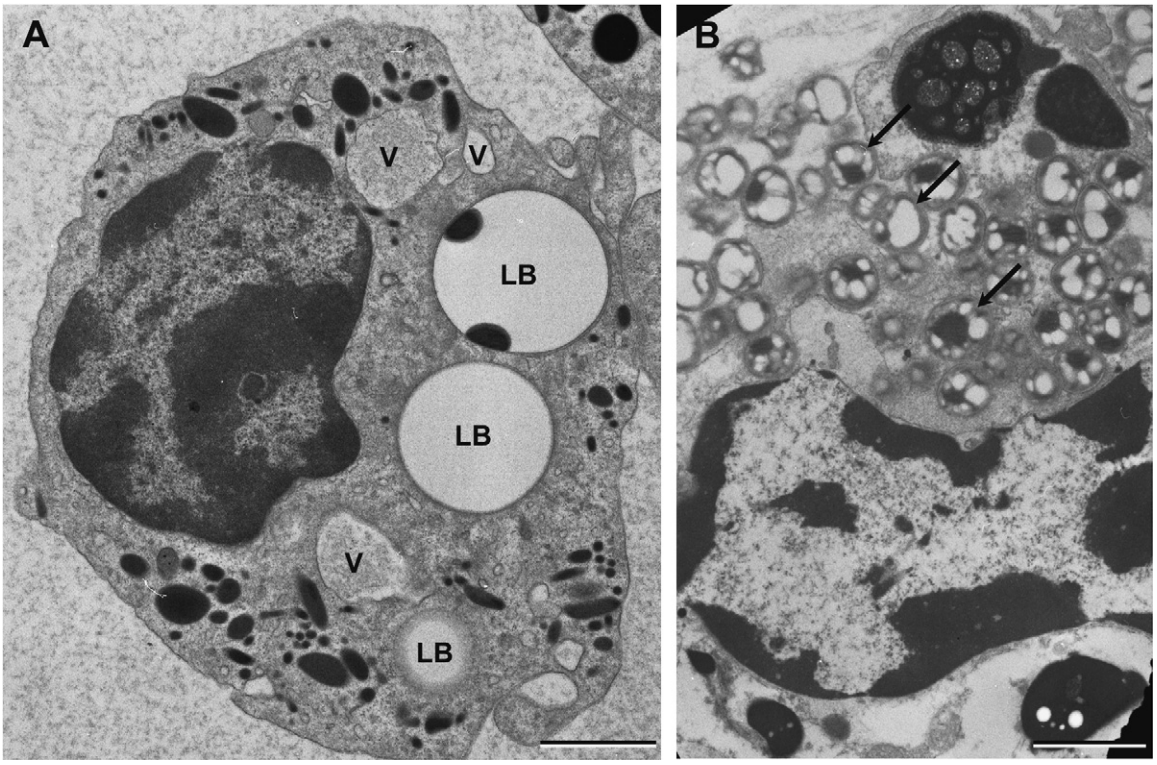

Fig. 6. Transmission electron microscopy of *A. leptodactylus* hemocytes after foreign particles injections. (A) Small granule hemocyte showing three phagosomes containing single 3 μm diameter latex bead (LB) 1 h after injection. Note several electron-lucent large vesicles in this activated cell (V). (B) Large granule hemocyte showing extensive phagocytic activity of 0.9 μm diameter carboxylated latex beads (arrows) 1 h after injection. Note the cytoplasm almost filled with latex particles and consequent cytolysis. Scale bars 2 μm (A and B).

from the hematopoietic tissue (Söderhäll et al., 2003). In *A. leptodactylus* we found L-DOPA PO reactivity in the granules of SGH, MGH and LGH and a strong activity in LGH cytoplasm (Fig. 5A and B) confirming this circulating hemocyte type as the major source of prophenoloxidase system in crustaceans.

As far as crustacean hemocytes phagocytosis activity is concerned, the phagocytosis assays of bacteria performed in vitro with *Homarus americanus*, *Panulirus interruptus* and *Loxorhynchus grandis* hemocytes revealed an involvement of both LGH and SGH with the strongest response of SGH with a maximum of 96% of phagocyting cells in this hemocyte category (Hose et al., 1990). In *Macrobrachium rosenbergii*, *M. acanthurus* and *Penaeus monodon* ''SGH and LGH, but apparently not the HH, were both able to engulf the yeast particles'' in vitro (Gargioni and Barracco, 1998). Surprisingly in another study the only hemocytes involved in latex beads phagocytosis in vitro are the hyaline cells (Sung and Ru Sun, 2002). These data are difficult to compare for the use of different particles and different methods to perform in vitro assays. Our approach tries to overcome these drawbacks by means of in vivo assays only with artificial beads with different diameters. In the in vivo phagocytosis assays all the hemocytes types were involved in the response but in *A. leptodactylus* the SGH is identified as the primary line of defense against foreign particles. In fact, following injection of all the latex beads, the SGH mounted the strongest phagocytic response as early as 30 min post-injection (Table 1).

After foreign particles treatments, the MGH presents only weak phagocytic activity with a maximum of 0.4% of total circulating hemocytes after 2 h of the injection of latex beads of 1 and 3 μm diameters. The percentages of these hemocytes during the in vivo treatments are rather constant even if the concomitant and extensive recruitment of LGH suggests an absolute low recruitment of this hemocyte type from hematopoietic tissues. The concomitant highest values of THC and LGH percentage in DHC 1 h post injection of carboxylated latex beads strongly suggest a primary role of LGH in acute inflammatory response with a rather rapid and massive recruitment of this type of hemocyte from hematopoietic tissues and/or from hemocelic storage compartments. Elicited proliferation in the hematopoietic tissue or from activated circulating stem cells is unlikely in our short-term study; as a matter of fact in the swimming crab *Liocarcinus depurator* lipopolysaccharide induces after 3 h a small proportion of circulating hemocytes to enter in S-phase in vitro and the authors suggest that this phase may last up to 20 h at 15 °C (Hammond and Smith, 2002).

Further study on long-term inflammatory response will elucidate if the recruitment of LGH is an acute response or a chronic response useful for crayfish health evaluation.

Acknowledgements

The authors are grateful to Mr. Claudio Gamboz and Prof. Maria Rosa Soranzo (Centro Servizi Polivalenti di Ateneo,

Trieste) for helpful suggestions and skilful technical support. We gratefully acknowledge Dr. Valerie J. Smith's helpful criticisms on the manuscript. We would like to express our sincere thanks to Dr. Stefano Sponza for the helpful discussions in statistical analysis. This research was supported by a regional grant LR FVG 3/1998 (''Valutazione delle condizioni di stress ambientale su popolazioni naturali e tecniche di allevamento finalizzate al ripopolamento del gambero di fiume *Austropotamobius pallipes italicus* del Friuli Venezia Giulia.'') to P.G.G.

References

Battison, A., Cawthorn, R., Horney, B., 2003. Classification of *Homarus americanus* hemocytes and the use of differential hemocyte counts in lobsters infected with *Aerococcus viridans* var. *homari* (Gaffkemia). J. Invert. Pathol. 843, 177–197.

Bauchau, A.G., 1981. Crustaceans. In: Ratcliffe, N.A., Rowley, A.F. (Eds.), Invertebrate Blood Cells, vol. 2. Academic Press, New York, pp. 386–420.

Chang, C.F., Chen, H.Y., Su, M.S., Liao, I.C., 2000. Immunomodulation by dietary beta-1, 3-glucan in the brooders of the black tiger shrimp *Penaeus monodon*. Fish Shellfish Immunol. 10, 505–514.

Gargioni, R., Barracco, M.A., 1998. Hemocytes of the palaemonids *Macrobrachium rosenbergii* and *M. acanthurus*, and of the penaeid *Penaeus paulensis*. J. Morphol. 236, 209–221.

Giulianini, P.G., Bertolo, F., Battistella, S., Amirante, G.A., 2003. Ultrastructure of the hemocytes of *Cetonischema aeruginosa* larvae (Coleoptera, Scarabaeidae): involvement of both granulocytes and oenocytoids in in vivo phagocytosis. Tissue Cell 35, 243–251.

Hammond, J.A., Smith, V.J., 2002. Lipopolysaccharide induces DNA-synthesis in a sub-population of hemocytes from the swimming crab, *Liocarcinus depurator*. Dev. Comp. Immunol. 26, 227–236.

Hillyer, J.F., Schmidt, S.L., Christensen, B.M., 2003a. Hemocyte-mediated phagocytosis and melanization in the mosquito *Armigeres subalbatus* following immune challenge by bacteria. Cell Tissue Res. 313, 117–127.

Hillyer, J.F., Schmidt, S.L., Christensen, B.M., 2003b. Rapid phagocytosis and melanization of bacteria and *Plasmodium* sporozoites by hemocytes of the mosquito *Aedes aegypti*. J. Parasitol. 89, 62–69.

Horney, B., Battison, A., MacKenzie, A., 2002. Cytocentrifuge preparations: an alternate method to examine the hemocytes of the American lobster, *Homarus americanus*. J. Shellfish Res. 21, 391.

Hose, J.E., Martin, G.G., Gerard, A.S., 1990. A decapod hemocyte classification scheme integrating morphology, cytochemistry, and function. Biol. Bull. 178, 33–45.

Johansson, M.W., Keyser, P., Sritunyalucksana, K., Söderhäll, K., 2000. Crustacean haemocytes and haematopoiesis. Aquaculture 191, 45–52.

Lorenzon, S., Francese, M., Smith, V.J., Ferrero, E.A., 2001. Heavy metals affect the circulating haemocyte number in the shrimp *Palaemon elegans*. Fish Shellfish Immunol. 11, 459–472.

Lorenzon, S., Pasqual, P., Ferrero, E.A., 2002. Different bacterial lipopolysaccharides as toxicants and stressors in the shrimp *Palaemon elegans*. Fish Shellfish Immunol. 13, 27–45.

Martin, G.G., Graves, B.L., 1985. Fine structure and classification of shrimp hemocytes. J. Morphol. 185, 339–348.

Mix, M.C., Sparks, A.K., 1980. Hemocyte classification and differential counts in the dungeness crab, *Cancer pagurus*. J. Invert. Pathol. 35, 134–143.

Perazzolo, L.M., Barracco, M.A., 1997. The prophenoloxidase activating system of the shrimp *Penaeus paulensis* and associated factors. Dev. Comp. Immunol. 21, 385–395.

Smith, V.J., Söderhäll, K., 1983. Induction of degranulation and lysis of haemocytes in the freshwater crayfish, *Astacus astacus* by components of the prophenoloxidase activating system in vitro. Cell Tissue Res. 233, 295–303.

Söderhäll, K., Smith, V.J., 1983. Separation of the haemocyte populations of *Carcinus maenas* and other marine decapods, and prophenoloxidase distribution. Dev. Comp. Immunol. 7, 229–239.

Söderhäll, I., Bangyeekhun, E., Mayo, S., Söderhäll, K., 2003. Hemocyte production and maturation in an invertebrate animal; proliferation and gene expression in hematopoietic stem cells of *Pacifastacus leniusculus*. Dev. Comp. Immunol. 27, 661–672.

Sung, H.H., Ru Sun, R.S., 2002. Use of monoclonal antibodies to classify hemocyte subpopulations of tiger shrimp (*Penaeus monodon*). J. Crustacean Biol. 22, 337–344.